

# DEVELOPMENT OF A FABRICABLE GAMMA-PRIME ( $\gamma'$ ) STRENGTHENED SUPERALLOY

L. M. Pike

Haynes International, 1020 West Park Ave., Kokomo, IN 46904-9013, USA

Keywords: wrought superalloy, alloy development, fabricability, weldability, strain-age cracking, creep-rupture

## Abstract

A recently developed wrought  $\gamma'$ -strengthened superalloy, HAYNES® 282® alloy, is introduced. The new alloy is a candidate for several high-temperature applications in both aero and land-based gas turbine engines. It is also being considered for aerospace structural components, as well as automotive and steam turbine applications. The metallurgical features of the new alloy are reported, and the relationship between these features and certain key properties of the alloy is discussed. It was found that carefully balancing the equilibrium amount of the  $\gamma'$  phase was crucial for producing an alloy which could be readily formed and welded, and yet still maintain exceptional creep strength. Too high levels of the  $\gamma'$  phase can lead to difficulties in fabrication, particularly the phenomenon of strain-age cracking. However, a certain amount of  $\gamma'$  is necessary for adequate creep, tensile, and fatigue strength. The  $\gamma'$  level in 282 alloy was optimized to achieve the best balance of strength and fabricability. Alloy properties such as creep, tensile, low-cycle fatigue, and thermal stability were presented for 282 alloy along with those of comparative alloys, R-41 alloy, Waspaloy alloy, and 263 alloy. The fact that 282 alloy was found to have equivalent or better mechanical properties compared to alloys with higher  $\gamma'$  content can be attributed in large part to the alloy's outstanding thermal stability.

## 1.0 Introduction

Wrought  $\gamma'$ -strengthened superalloys which can be conventionally hot and cold worked are found in numerous applications in aero and land-based gas turbine engines. Such applications include combustors, transitions, rings, nozzles, cases, etc. Of critical importance for alloys used in such parts is fabricability, that is the capacity to be both readily welded and formed into various shapes. As will be discussed, the equilibrium amount of  $\gamma'$  phase has a strong influence on both of these characteristics. Generally, a lower  $\gamma'$  content is desired for improved formability as well as weldability. However, a lower  $\gamma'$  content is not so desirable for mechanical properties, such as higher creep and tensile strength. Therefore, the challenge of developing a new wrought  $\gamma'$  strengthened alloy is to determine a composition which optimizes high temperature strength, while at the same time allowing for successful fabrication.

HAYNES 282 alloy has recently been developed for high temperature structural applications [1]. The new alloy possesses a unique combination of creep strength, thermal stability, and fabricability not found in currently available commercial alloys. The new alloy has excellent creep strength in the temperature range of 1200 to 1700°F (649 to 927°C), surpassing that of Waspaloy alloy and approaching that of R-41 alloy. This level of creep strength was obtained despite the alloy having a

significantly lower volume fraction of the strengthening  $\gamma'$  phase. Since its introduction in fall of 2005, the 282 alloy has received considerable attention being selected for applications in both aero and land-based gas turbine engines and is the subject of several test programs being conducted by both industrial and governmental organizations. The purpose of this paper will be to introduce the key metallurgical features of 282 alloy and discuss their implications on the fabricability and mechanical properties of this promising new alloy.

## 2.0 Metallurgical Features of 282 Alloy

### 2.1 Composition

The composition of HAYNES 282 alloy is shown in Table I along with three other wrought  $\gamma'$ -strengthened alloys in its class. All four alloys are nickel-base and contain similar alloying additions. The presence of 19 to 20 wt.% Cr is important to provide resistance to both oxidation and hot corrosion, while Co is used to control the  $\gamma'$  solvus. In 282 alloy, the level of Co, a relatively costly element, is on the low end of the usual range for this class of alloys, typically 10 to 20 wt.%. An important element for providing creep strength is Mo, present in these alloys from 4.3 to 10 wt.%. The critical role of Mo in providing 282 alloy with excellent creep strength will be further elaborated on in Section 2.5. The elements Al and Ti are the  $\gamma'$  forming elements. Small changes in the amount of these two elements have strong effects on the properties and fabricability of these alloys. Consequently, the Al and Ti levels in 282 alloy were carefully selected to provide the best combination of these traits. The important role of Al and Ti will be discussed in more detail in Section 2.4.

Minor alloying additions such as C and B were added to 282 alloy to provide improved mechanical properties. These minor additions are also found in the other three alloys. Only Waspaloy alloy has an intentional Zr addition. This element is believed to provide grain boundary strengthening in some alloys [2], but is often known to cause problems with hot cracking during welding. For this reason Zr is not included in Waspaloy filler metal. The elements Mn and Si are intentionally added to 263 alloy, presumably for oxidation resistance and/or castability. These elements are not added to 282, R-41, or Waspaloy alloys, yet the oxidation resistance of all four has been found to be very similar in a recent study [3]. Moreover, Mn and Si are not desirable from the standpoint of thermal stability (lead to high Nv values).

### 2.2 Solution Annealing

A full solution annealing treatment is typically given to 282 alloy after fabrication. The solution annealing temperature is normally in the range of 2050 to 2100°F (1121 to 1149°C). A rapid cool is preferred for optimum properties. In the annealed condition, sheet

Table I Nominal Composition of Several Wrought Gamma-Prime Alloys (wt.%)

Alloy	Ni	Cr	Co	Mo	Ti	Al	Fe	Mn	Si	C	B	Other
282	57 <sup>a</sup>	20	10	8.5	2.1	1.5	1.5*	0.3*	0.15*	0.06	0.005	--
Waspaloy	58 <sup>a</sup>	19	13.5	4.3	3	1.5	2*	0.1*	0.15*	0.08	0.006	Zr-0.05
R-41	52 <sup>a</sup>	19	11	10	3.1	1.5	5*	0.1*	0.5*	0.09	0.006	--
263	52 <sup>a</sup>	20	20	6	2.4*	0.6*	0.7*	0.4	0.2	0.06	0.005	Al+Ti-2.6

<sup>a</sup>As Balance

\*Maximum

or plate material of 282 alloy would typically have an ASTM grain size of approximately 4 to 4½. A micrograph of 282 alloy in the solution annealed condition is shown in Fig. 1. The product form is 0.062" (1.6mm) sheet. The solution annealing temperature is above the solvus of the M<sub>23</sub>C<sub>6</sub> carbide. Therefore, the grain boundaries are seen to be clean and the grain interiors free of secondary precipitation. However, large, blocky primary titanium-rich MC carbides can be observed. If cooled with sufficient rapidity, little, if any, γ' phase will be present in 282 alloy after solution annealing and the material will be soft and ductile. Further discussion of the as-annealed properties of 282 alloy as they relate to fabricability will be discussed in Section 4.

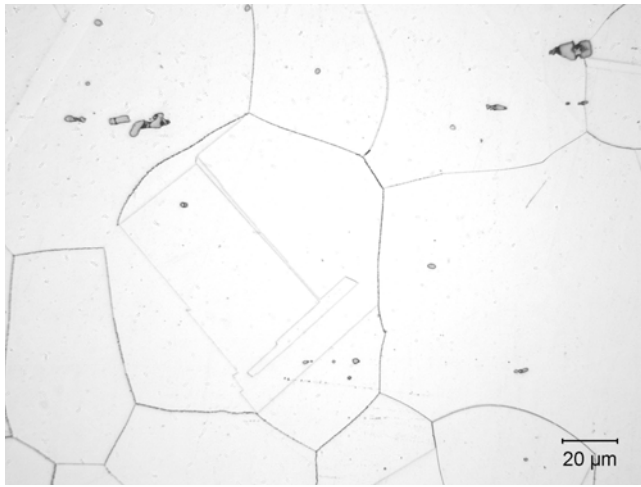


Fig. 1 Mill annealed microstructure of 282 alloy

### 2.3 Precipitation Heat Treatment

After solution annealing, 282 alloy is given a two-step heat treatment of 1850°F (1010°C) /2h/AC + 1450°F (788°C)/8h/AC. The resulting microstructure is shown in Fig. 2. Compared to the solution annealed condition, the presence of both secondary intragranular and grain boundary precipitation can be observed. No γ' precipitates can be seen at this low magnification. The first step of the heat treatment is above the γ' solvus temperature of 1827°F (997°C) and, therefore, does not result in strengthening. The purpose of the first step of the heat treatment is believed to be the formation of chromium-rich M<sub>23</sub>C<sub>6</sub> carbides at the grain boundaries in the most preferred morphology for optimum mechanical properties. Indeed, an improvement in both creep strength and high temperature ductility has been found to result from the application of this first step as part of the heat treatment process. An SEM image of the grain boundary structure in as-heat treated 282 alloy is shown in Fig. 3. The sample was etched to preferentially attack the near-boundary region and thus reveal

the nature of the grain boundary precipitates, which appear in a blocky "stone wall" configuration.



Fig. 2 Age-hardened microstructure of 282 alloy

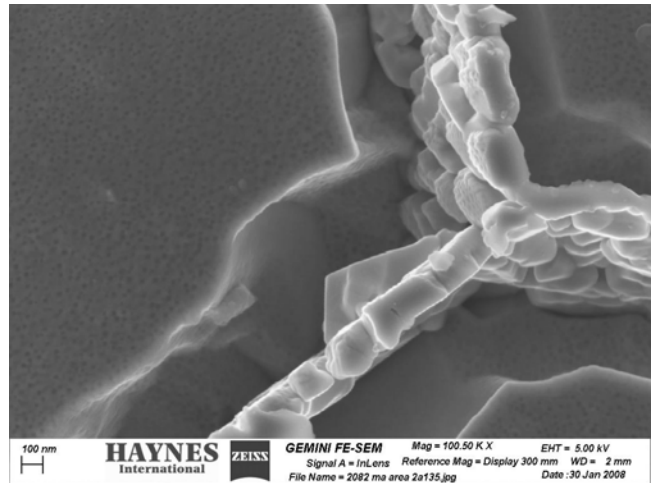


Fig. 3 Grain boundary structure in 282 alloy

The second step of the heat treatment results in the formation of the γ' phase. In the as-heat treated condition, the γ' is roughly spherical and very fine in size with a diameter of approximately 20nm. An SEM image of the γ' precipitation is shown in Fig. 4. The distribution and size of the γ' particles is seen to be quite uniform. Another SEM image showing both the grain boundary precipitation and γ' precipitates is shown in Fig. 5.

### 2.4 γ' Phase Fraction

The equilibrium fraction of the γ' phase has significant implications on both mechanical properties and fabricability. Higher levels of γ' are desirable for high strength, both creep and tensile. However, lower γ' levels are necessary for improved

fabricability. For this reason, the amount of  $\gamma'$  in 282 alloy was carefully balanced. The strongest compositional factor controlling the amount of  $\gamma'$  phase is the amount of Al and Ti, best expressed in terms of atomic percent as shown in Table II for several  $\gamma'$ -strengthened alloys. It can be seen that the total Al + Ti content for 282 alloy falls between 263 alloy (readily fabricable, but low strength) and the Waspaloy and R-41 alloys (higher strength than 263 alloy, but much less fabricable). The same can be said for the equilibrium  $\gamma'$  phase fraction of 282 alloy, also given in Table II. The calculations were performed for equilibrium at 1400°F (760°C) for the four alloys using PANDAT v. 5.0 software combined with the Ni-Data v.7 thermodynamic database. The calculated phase fraction for 282 alloy was 19%, which was between 263 alloy (12%) and the Waspaloy and R-41 alloys (24 and 27%, respectively). The intermediate level of equilibrium  $\gamma'$  allows 282 alloy to have exceptional fabricability, while also possessing excellent strength.

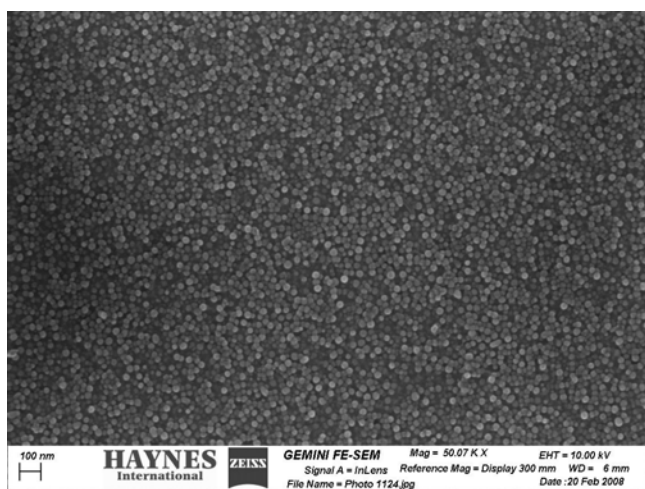


Fig. 4 Gamma-prime phase distribution in 282 alloy

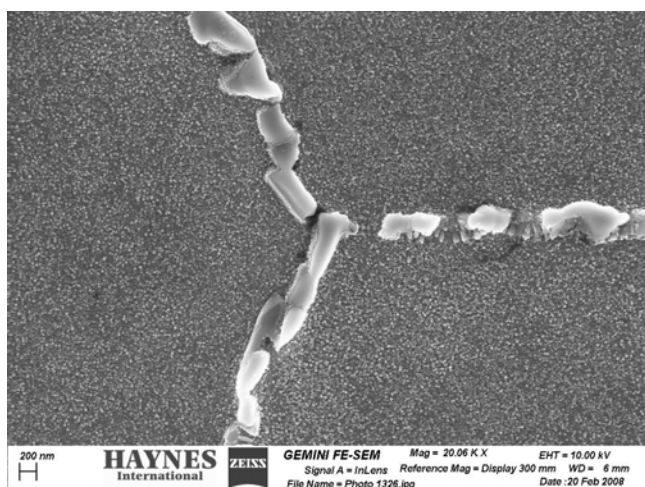


Fig. 5 Grain boundary triple junction in 282 alloy

### 2.5 Mo Effect

Molybdenum is an important element in determining the creep strength of wrought  $\gamma'$  strengthened alloys. Being a relatively large and immobile atom, Mo provides significant solid-solution

strengthening and for this reason is present in all four of the alloys in Table I. During the development of 282 alloy it was found that increasing amounts of Mo generally led to greater creep strength. However, this trend did not hold indefinitely. Consider the creep-rupture data shown in Fig. 6 which came from tests performed at 1700°F (927°C) at 13 ksi (90 MPa). In this plot, the rupture life is plotted as a function of the Mo content, with all other alloying elements held constant. The rupture life was found to increase with increasing Mo content up to around 8.5 wt.% (the nominal Mo level in 282 alloy). With additional increases in Mo the rupture life decreased rapidly. Further work is underway to confirm the mechanism behind this strong Mo effect.

Table II Percentages of the Gamma-Prime Phase and Gamma-Prime Forming Elements

Alloy	Gamma-Prime Forming Elements (at.%)			Calculated Equilibrium Gamma-Prime Phase at 1400°F (760°C) (mole %)
	Al	Ti	Al + Ti	
263 alloy	1.2	2.6	3.8	12
282 alloy	3.1	2.5	5.6	19
Waspaloy alloy	3.1	3.5	6.6	24
R-41 alloy	3.3	3.8	7.1	27

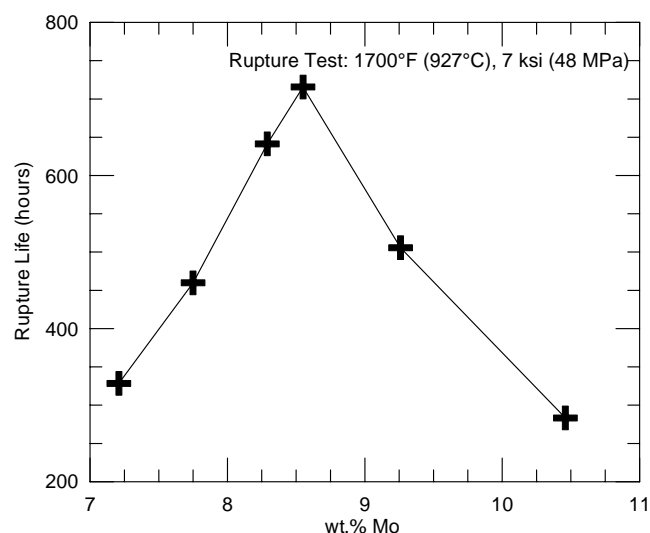


Fig. 6 Effect of Mo on the creep-rupture strength of 282 alloy

### 3.0 Heat Treatments of Comparative Alloys

The mill annealing and age-hardening heat treatments applied to the comparative alloys discussed in this manuscript are given in Table III. These include R-41, Waspaloy, and 263 alloys. Note that R-41 alloy has two popular age-hardening treatments applied after mill annealing at 1975°F (1079°C): 1) 2050°F (1121°C)/2h/AC + 1650°F (899°C)/4h/AC, and 2) 1400°F (760°C)/16h/AC. In this study all testing was performed using the former of these aging treatments. This heat treatment provides improved creep strength, but lower yield and ultimate tensile strength relative to the second aging treatment. It also results in an unusual duplex grain size of ASTM 2-5. Waspaloy, 282, and

Table III Annealing and Age-Hardening Heat Treatments and Grain Size

Alloy	282 Alloy	Waspaloy alloy	R-41 alloy	263 alloy
Mill Annealing Temperature	2100°F (1149°C) <sup>b</sup>	1975°F (1079°C) <sup>o</sup>	1975°F (1079°C) <sup>o</sup>	2100°F (1149°C) <sup>b</sup>
Age-Hardening Heat Treatment	1850°F (1010°C)/2h/AC + 1450°F (788°C)/8h/AC	1825°F (996°C)/2h/AC + 1550°F (843°C)/4h/AC + 1400°F (760°C)/16h/AC	2050°F (1121°C)/0.5h/RAC + 1650°F (899°C)/4h/AC	1472°C (800°C)/8h/AC
ASTM Grain Size	4½	5	5 (as MA) 2-5 (after age-hardening)	4

<sup>o</sup>Oxidize anneal

<sup>b</sup>Bright anneal

AC = Air cool

RAC = Rapid air cool (fan cool)

263 alloys have grain sizes in the range of ASTM 4 to 5 which are unaffected by the age-hardening heat treatments.

#### 4.0 Relationship of $\gamma'$ and Fabricability

##### 4.1 $\gamma'$ Precipitation Kinetics

The equilibrium level of  $\gamma'$  strongly affects the precipitation kinetics of the phase, with higher levels leading to greatly accelerated precipitation. In an effort to compare the  $\gamma'$  precipitation kinetics of 282 alloy to other alloys in its class, the hardness of samples originally in the solution annealed condition was measured after isothermal exposures of varying duration at 1300, 1500, and 1700°F (704, 816, and 927°C). The samples were made of 0.063" (1.6 mm) sheet to enable fast heat up rates, and samples were water quenched at the end of their exposure duration. The solution annealed hardness values were 55, 57, 58, and 64 Ra for 263, 282, Waspaloy, and R-41 alloys, respectively. (Note the high hardness of R-41 alloy in the solution annealed condition suggests the presence of  $\gamma'$  due to insufficient cooling – more on this in Section 4.3.) The hardening responses to the isothermal exposures are shown in Fig. 7. The highest hardness values were achieved in samples aged at 1500°F (816°C). At this temperature, the two alloys with higher  $\gamma'$  content (R-41 alloy and Waspaloy alloy) were found to harden very rapidly, with Waspaloy achieving a hardness level of 62 Ra in less than 2 minutes, and of 66 Ra in less than 5 minutes. R-41 alloy hardened at an even faster rate. Conversely, the 282 alloy was found to harden more sluggishly, similar to 263 alloy, a material known for its ease of fabricability. These two alloys did not achieve hardness levels of 62 Ra for more than 20 minutes. For R-41 and Waspaloy alloys, the precipitation kinetics were even more rapid at 1700°F (927°C). At this temperature both alloys achieved a hardness of 62 Ra in less than 1 minute. For 282 alloy, however, the hardening response was much more gradual at this temperature. The 263 alloy hardened very minimally at this temperature and began to overage after 100 minutes. The most sluggish hardening in R-41, Waspaloy, and 282 alloys was seen at the lowest temperature in the study, 1300°F (704°C).

The relative ranking of the  $\gamma'$  precipitation kinetics remained the same in a similar study shown in Fig. 8. In this study, isothermal exposures were conducted at temperatures ranging from 1000 to 1900°F (538°C to 1038°C) for varying durations. The results are plotted as T-T-H curves for each of the four alloys. The curves correspond to a Rc hardness of 30. The results indicate that 282 alloy has considerably more sluggish precipitation kinetics than either R-41 or Waspaloy alloys, while being slightly more rapid than 263 alloy. This has profound implications on fabricability as will be discussed in the following two sections of this paper.

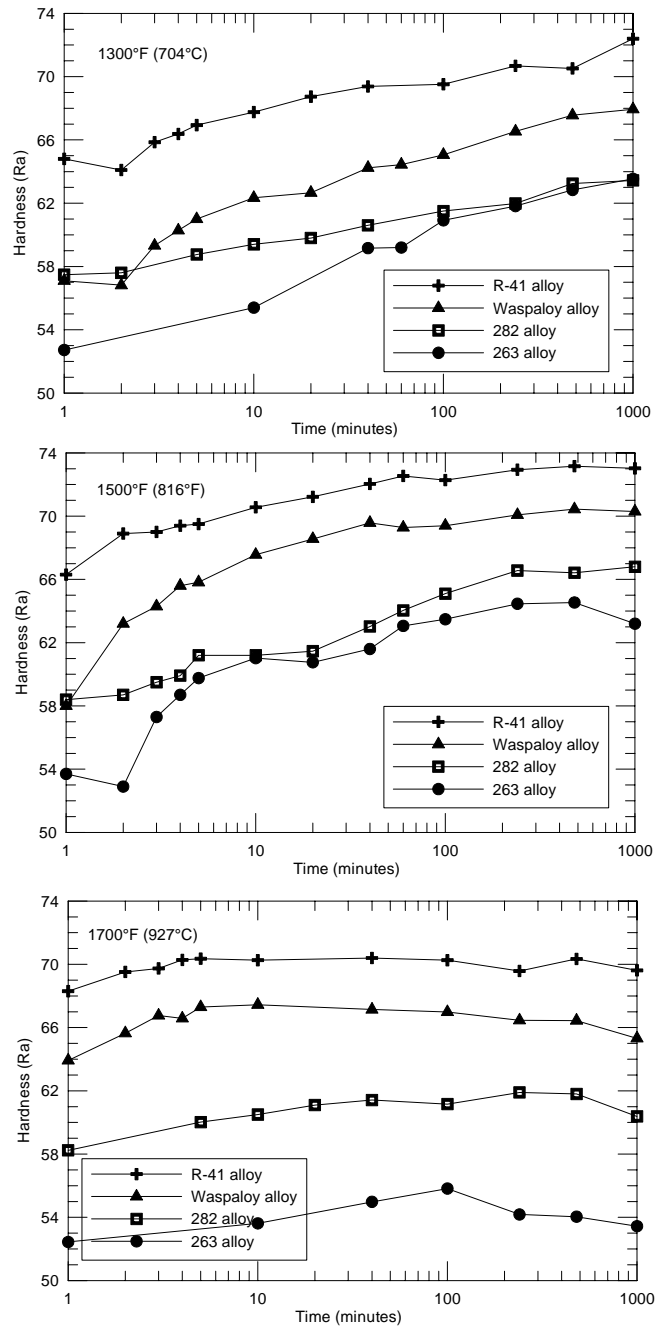


Fig. 7 Isothermal hardening at 1300°F (704°C), 1500°F (816°C), and 1700°F (927°C).

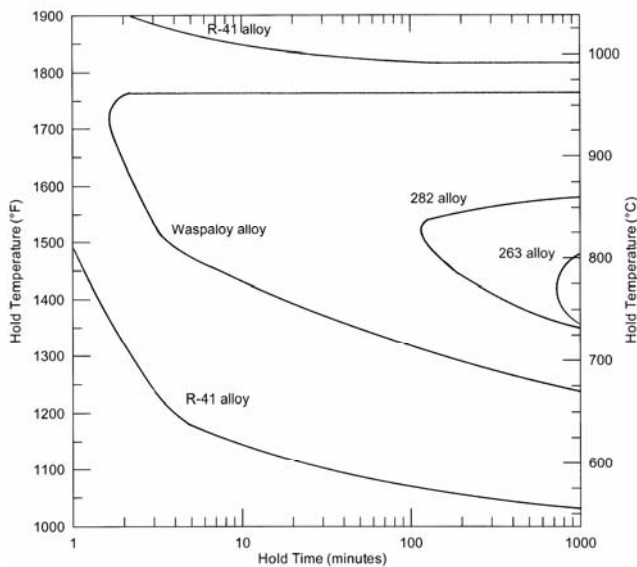


Fig. 8 T-T-H curves corresponding to 30Rc

#### 4.2 Strain-Age Cracking

A major effect resulting from the precipitation of  $\gamma'$  during component fabrication is the issue of strain age-cracking, a problem which plagues a number of “weldable”  $\gamma'$ -strengthened alloys. Strain-age cracking typically occurs during heat up in the first post-weld heat treatment (usually a solution anneal) of a welded component. The cracking has been associated with residual stresses in the material which are created by solidification shrinkage coupled with the formation of  $\gamma'$  during the heat treatment. Therefore, alloys which have faster  $\gamma'$  precipitation kinetics are much more likely to be susceptible to this form of cracking. A useful test to determine an alloy's resistance to strain-age cracking is the controlled heating rate tensile (CHRT) test developed at Rocketdyne in the late 1960's [4]. The CHRT test was found to successfully identify individual heats of R-41 alloy which had greater susceptibility to strain age cracking as determined using the more difficult and costly circular patch test. More recently, a study of several  $\gamma'$  strengthened sheet alloys was conducted by M.D. Rowe at Haynes International [5]. In the CHRT test, the sample is heated to the test temperature at a rate chosen to simulate the heat up during the first heat treatment after welding. The sample is originally in the solution annealed condition (little to no  $\gamma'$  present) so that  $\gamma'$  precipitates continuously during the test. A range of test temperatures are chosen (typically between 1400 and 1600°F (760 to 871°C)) and the strain-age cracking resistance of the alloy is taken as the minimum elongation in that temperature range. An advantage of the CHRT test over other test methods for evaluating susceptibility of alloys to strain-age cracking is that it has a quantitative result (minimum elongation) which can be used to compare alloys, rather than a less useful pass/fail result.

Controlled heating rate tensile tests were performed on three different production scale heats of 282 alloy sheet. For consistency with the study of Rowe [5] all testing was done on 0.063” (1.6 mm) sheet. The results are shown in Fig. 9, where each data point represents an average of duplicate tests on each of

the three heats. Also shown in Fig. 9 are the data from the Rowe study for R-41, Waspaloy, and 263 alloys. In the plot, it is evident that the R-41 and Waspaloy alloys (both of which are well known to be susceptible to strain-age cracking [6]) have minimum elongations less than 5%. In contrast, 282 alloy has a minimum CHRT elongation of 13% at 1500°F (816°C), which suggests the alloy is very resistant to strain-age cracking. The 263 alloy had the best performance of the four alloys in the CHRT test, as might be expected from its reputation as being readily weldable [7]. The results are in good agreement with the relative ranking of the  $\gamma'$  precipitation kinetics as described in the previous section. The predicted weldability of 282 alloy has since been corroborated by the reported field experiences of more than one OEM.

The potential for strain-age cracking in susceptible alloys limits the thickness of the components produced using the alloy. For example, applications requiring flat products of Waspaloy and R-41 alloys are generally limited to sheet gauges, while 282 and 263 alloys are readily welded as thick plate as well as thinner plate and sheet products.

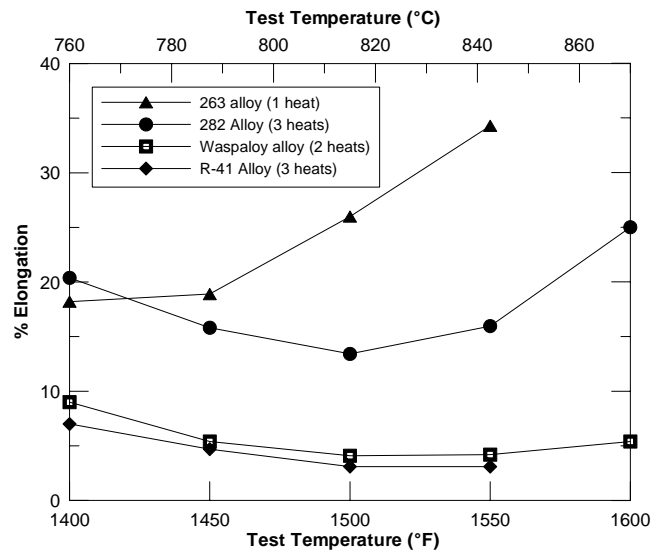


Fig. 9 Comparative CHRT ductility

#### 4.3 Formability After Intermediate Annealing

Another important aspect of fabrication which is strongly affected by the rate of  $\gamma'$  precipitation is intermediate annealing treatments. These heat treatments are generally given to restore the material to the soft and ductile condition following hot or cold work. Such a condition is necessary to allow the material to be further worked or formed. However, for some  $\gamma'$  strengthened alloys it is difficult to achieve this soft and ductile condition even after solution annealing. This can be attributed to the formation of the  $\gamma'$  phase during the post-anneal cooling, resulting in increased stiffness and reduced ductility. For this reason this class of alloys is often rapidly cooled or water-quenched after annealing. However, for alloys with very rapid  $\gamma'$  precipitation kinetics, such as R-41 or Waspaloy alloys, even water quenching may not be sufficiently rapid to completely prevent  $\gamma'$  precipitation. To illustrate this, consider the mill annealed tensile data of several alloys given in Table IV. The data in this table were generated from a large

number of production heats of sheet material ranging from 0.060 to 0.125" (1.5 to 3.2 mm). The 282 and 263 alloys are seen to have much lower strength and higher ductility than the Waspaloy and R-41 alloys. This suggests significantly greater formability for the former two alloys. This distinction is even more significant considering the fact that the 282 and 263 sheets are mill annealed using a process known as "bright annealing" in which a continuous coil is annealed in a hydrogen atmosphere (leaving the material with a desirable shiny surface finish). However, this process does not lend itself to water quenching so the cooling rate after annealing is relatively slow. The R-41 and Waspaloy alloys cannot be produced in this manner, and must instead be "black annealed" (in air) and water quenched, a more time consuming and costly processing route. Despite these precautions, it is clear from the data in Table IV that both alloys still form  $\gamma'$  phase during cooling leaving them in a less formable condition. As with strain-age cracking, the issue of formability after intermediate heat treatments also limits the thickness from which components can be fabricated out of  $\gamma'$ -strengthened alloys.

Table IV Mill Annealed Tensile Properties

Alloy	0.2% Yield Strength		Ultimate Tensile Strength		Elongation %
	ksi	MPa	ksi	MPa	
282 alloy	56	385	122	839	59
263 alloy	48	327	116	798	58
Waspaloy alloy	71	490	135	930	46
R-41 alloy	86	592	152	1047	39

## 5.0 Key Properties of 282 Alloy

### 5.1 Creep-Rupture

Extensive creep-rupture testing has been performed on sheet and plate forms of 282 alloy with plate samples generally having somewhat longer rupture lives under identical test conditions. For the purposes of this paper, the focus will be on the testing of sheet products since comparative alloy data are more readily available. The creep-rupture testing was performed at temperatures ranging from 1200 to 1700°F (649 to 927°C) on 0.023 to 0.125" (0.6 to 3.2 mm) thick sheet samples. To date, a total of 32 tests have been completed on samples from three different production heats and six different thickness levels. A Larson-Miller plot of both 1% creep and rupture data for 282 alloy is given in Fig. 10. From the data, the stress values required to produce 1% creep and rupture in 1000h were determined and are given in Table V along with such values for age-hardened R-41, Waspaloy, and 263 alloys. Of the four alloys, 263 alloy had the lowest creep and rupture strength across the entire temperature range. The rupture strengths of 282 and Waspaloy alloys are about the same at 1200 to 1300°F (649 to 704°C), but at higher temperatures 282 alloy has a distinct advantage. In terms of 1% creep, the 282 alloy was found to be significantly stronger than Waspaloy alloy over the entire temperature range of 1200 to 1700°F (649 to 927°C). When compared to R-41 alloy, the 282 alloy had a lower rupture strength in the temperature range of 1200 to 1400°F (649 to 760°C), but the two alloys had very similar rupture strength at temperatures of 1500°F (816°C) and greater. Similarly, the R-41

alloy had slightly higher 1% creep strength at 1200 to 1400°F (649 to 760°C). Again, however, the distinction between 282 alloy and R-41 alloy disappeared at higher temperatures, with the 1% creep strength of the two alloys being virtually the same at temperatures of 1500°F (816°C) and greater. This can be seen clearly in Fig. 11, in which the 1% creep lives of 282, R-41, Waspaloy, and 263 alloys are shown in a Larson-Miller plot. The plot shows experimental data points for samples tested between 1500 and 1700°F (816 and 927°C). In this plot it is seen that 282 and R-41 alloys have virtually the same creep strength, while both alloys are clearly stronger than Waspaloy and 263 alloys.

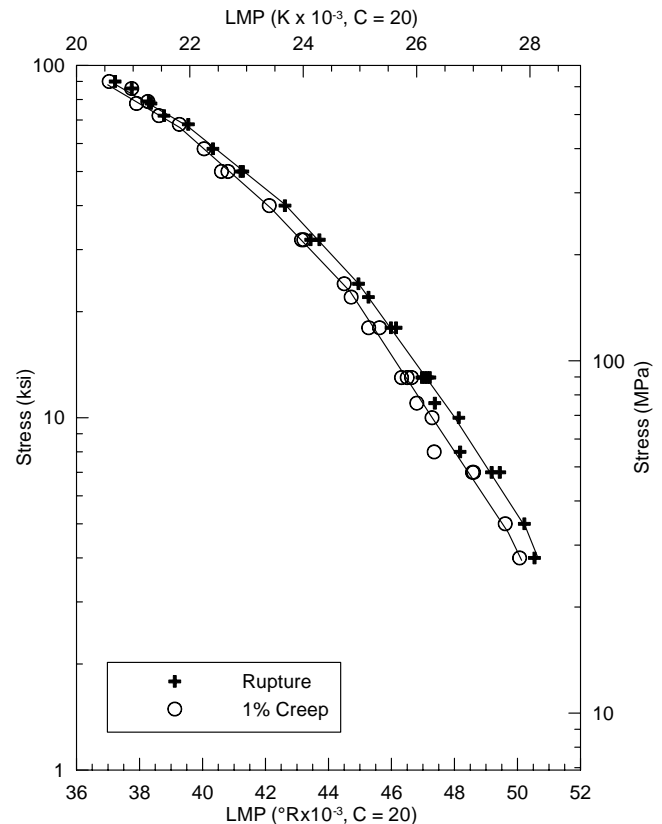


Fig. 10 Larson-Miller plot of rupture and 1% creep for 282 alloy

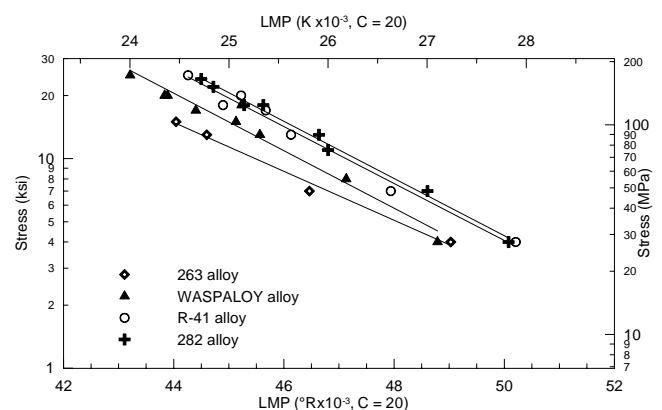


Fig. 11 Comparative 1% creep, 1500 to 1700°F (816 to 927°C)

Table V Stress to Produce 1% Creep and Rupture in 1000 Hours - Sheet

Property	Test Temperature		263 Alloy		R-41 Alloy		Waspaloy Alloy		282 Alloy	
	°F	°C	ksi	MPa	ksi	MPa	ksi	MPa	ksi	MPa
Stress-to-Produce 1% Creep, in 1000 h ksi (MPa)	1200	649	58	400	84	579	67	462	79	545
	1300	704	41	283	59	407	46	317	53	365
	1400	760	25	172	34	234	28	193	35	241
	1500	816	12	83	18	124	16	110	21	145
	1600	871	6	41	9	62	7	48	10	69
	1700	927	3	21	5	34	3	21	5	34
Stress-to-Produce Rupture, in 1000 h ksi (MPa)	1200	649	64	441	90	621	80	552	80	552
	1300	704	45	310	68	469	58	400	56	386
	1400	760	28	193	43	296	36	248	38	262
	1500	816	15	103	24	165	20	138	23	159
	1600	871	7	48	13	90	10	69	12	83
	1700	927	4	28	7	48	3	21	6	41

5.2 Tensile

Tensile testing was performed at temperatures ranging from RT to 1800°F (982°C) on six thicknesses of 282 alloy sheet from three different production scale heats. The average yield strength of 282 alloy as a function of temperature is shown in Fig. 12. The yield strength decreased only gradually from room temperature up to around 1400°F (760°C). At temperatures between 1400 and 1600°F (760 and 871°C), the decline in the yield strength with temperature was more rapid, but still relatively gradual. However, at temperatures greater than 1600°F (871°C) the yield strength dropped rapidly with increasing temperature.

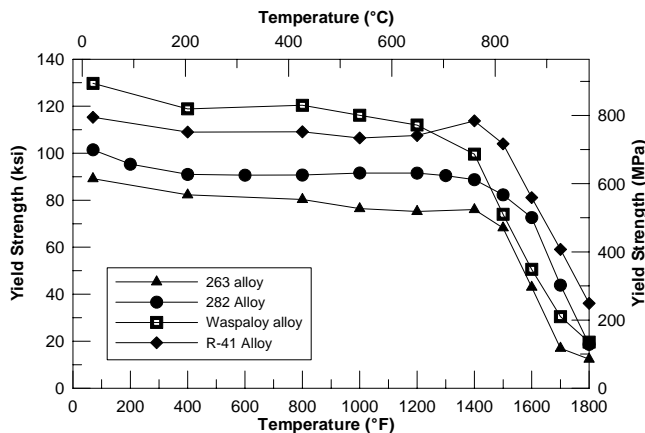


Fig. 12 Comparative tensile yield strength data

Also shown in Fig. 12 is the yield strength of sheet products of R-41, Waspaloy, and 263 alloys. At room temperature, the yield strength of 282 alloy was lower than that of R-41 and Waspaloy alloys, but greater than that of 263 alloy. As with 282 alloy, the yield strengths of R-41, Waspaloy, and 263 alloys decreased only slightly with temperature up to 1400°F (760°C). However, at greater temperatures the yield strength of both Waspaloy and 263 alloys dropped off sharply with increasing temperature. Only R-41 alloy exhibited the more gradual decrease in the 1400 to

1600°F (760 to 871°C) range as was seen for 282 alloy. With the sharp drop in yield strength of Waspaloy above 1400°F (760°C), the relative strength of the alloys changed with 282 alloy having greater strength than Waspaloy alloy at 1500°F (816°C) and above.

The average tensile elongation of 282 alloy is shown in Fig. 13 as a function of temperature. The elongation was found to slightly increase with temperature up to around 1000°F (538°C). An intermediate temperature ductility minimum was observed between 1000 and 1700°F (538 and 927°C), with a minimum of 22% at 1400°F (760°C). At greater temperatures the elongation increased rapidly. The elongations of R-41, Waspaloy, and 263 alloys are also plotted in Fig. 13. The elongation of 263 alloy was quite high, exhibiting a minimum ductility at 1400°F (760°C) at 27%. The elongations of Waspaloy and R-41 alloys were somewhat lower at room temperature than 282 or 263 alloys, a trend which extended out to around 1000°F (538°C). At higher temperatures the elongations of both alloys increased and thus did not exhibit an intermediate temperature ductility minimum.

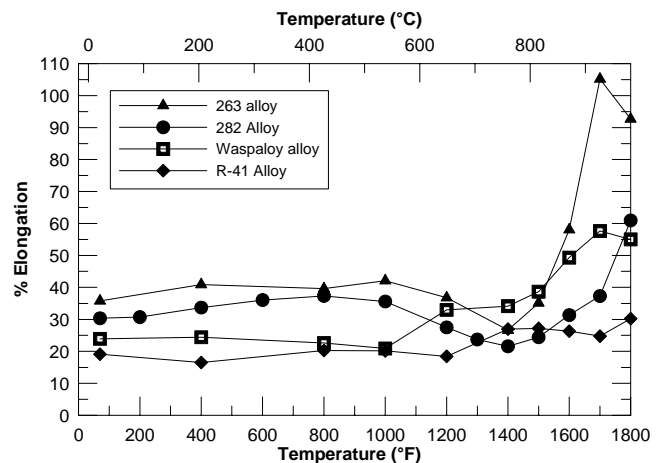


Fig. 13 Comparative tensile elongation data

### 5.3 Low Cycle Fatigue (LCF)

The LCF behavior of 282 alloy was the subject of a recent study [8]. The testing was conducted using fully-reversed strain-control over a temperature range of 1200°F (649 to 871°C). The results are shown in Fig. 14. The LCF resistance was found to gradually increase with temperature up to 1500°F (816°C). Above this temperature, the LCF resistance decreased more rapidly.

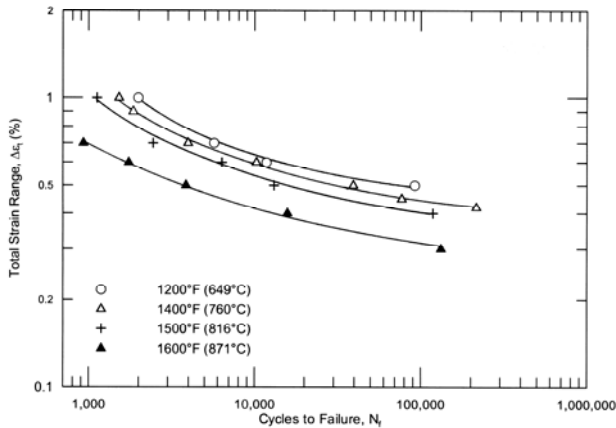


Fig. 14 LCF behavior of 282 alloy at various temperatures

The LCF behavior of the three comparative wrought superalloys was also investigated at 1500°F (816°C). The results are shown in Fig. 15. At lower total strain ranges, the R-41 alloy had the best LCF resistance followed by Waspaloy and 282 alloy, in that order. However, at higher total strain ranges, 282 alloy, Waspaloy alloy, and R-41 alloy were found to have nearly identical LCF resistance. The 263 alloy had the lowest LCF resistance at all strain ranges of the four alloys in the study.

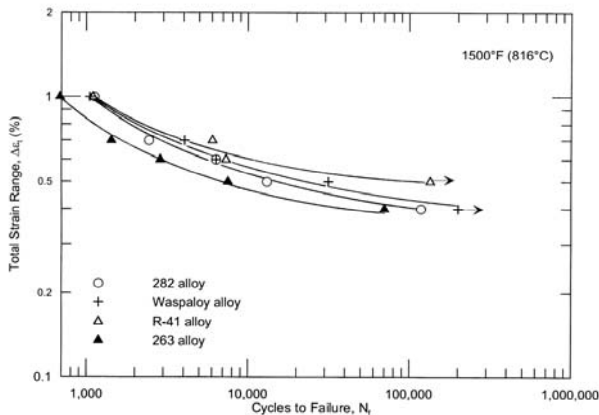


Fig. 15 Comparative LCF data at 1500°F (816°C)

### 6.0 Thermal Stability

For high temperature materials, the stability of the microstructure over long term thermal exposures can have important effects on material properties. In many alloys, such thermal exposures can lead to formation of deleterious phases such as  $\sigma$  and  $\mu$  phase.

These phases can lead to a significant loss of room temperature ductility, as well as elevated creep-rupture strength [2]. In  $\gamma'$ -strengthened alloys, a second undesired effect of thermal exposure can be the coarsening or over-aging of the  $\gamma'$  precipitates. Such coarsening can lead to loss of strength, both tensile and creep [2]. Haynes 282 alloy was designed to be resistant to both forms of thermal instability, as will be discussed in the following two sections.

### 6.1 Thermal Exposures: RT Ductility

Loss of retained room-temperature ductility is a good indicator of the formation of deleterious phases which also may affect high temperature strength. The thermal stability of 282 alloy was investigated using thermal exposures of 1000 hours at temperatures of 1200, 1400, 1500, and 1600°F (650, 760, 816, and 871°C). The thermal exposures were applied to material initially in the age-hardened condition. After the thermal exposure, samples were given a room temperature tensile test to determine their retained ductility. The results are shown in Fig. 16 as elongation vs. exposure temperature. In this plot, the elongation values for the “RT exposure” were simply taken as the corresponding elongation in the as-age hardened condition. The retained ductility for 282 alloy was found to be greater than 20% for all four exposure temperatures, suggesting that it has good thermal stability at least out to 1000 hours.

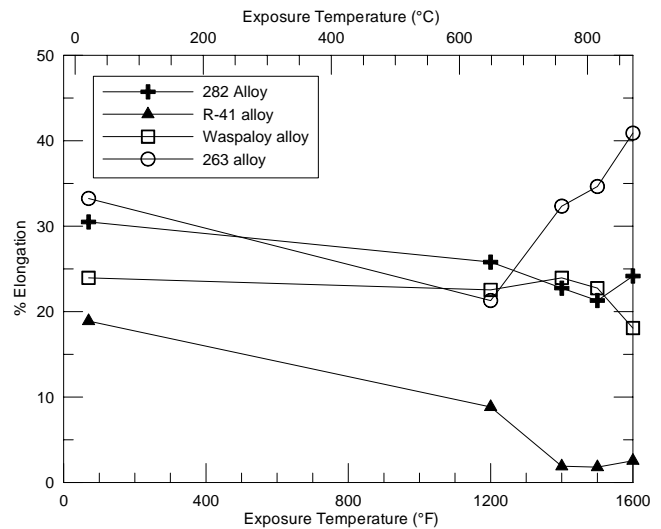


Fig. 16 Comparative retained ductility after 1000 hour thermal exposure

For comparison, thermal stability testing was conducted on sheet material of R-41, Waspaloy, and 263 alloys across the same temperature range. The results are also given in Fig. 16. A dramatic loss of retained ductility was observed for R-41 alloy, particularly for exposures at 1400°F (760°C) and above. This embrittlement resulted from the formation of the brittle  $\sigma$  and  $\mu$  phases, which have been reported by other investigators to be present in thermally exposed R-41 alloy [9-11]. The retained ductility of Waspaloy alloy remained relatively constant at exposure temperatures up to 1500°F (816°C), but decreased to around 18% at 1600°F (871°C). Finally, the retained ductility of 263 alloy decreased from 33% down to 21% after exposure at 1200°F (649°C). At 1400 and 1500°F (760 and 816°C), the



retained ductility was relatively unchanged over the as-age hardened condition. After exposure at 1600°F (871°C), the ductility was found to increase along with a sharp decrease in yield strength, likely a result of  $\gamma'$  coarsening.

## 6.2 Thermal Exposures: Strength

To study the effect of thermal exposure on the strength of the 282 alloy, samples exposed for 1000 hours at 1400°F (760°C) were subjected to tensile testing *at the exposure temperature*. In this way the thermal stability under service conditions could be best be evaluated. The yield strength of the thermally exposed material is shown in Fig. 17 along with that of the as-age hardened material. For 282 alloy the yield strength was found to increase from 87 ksi (598 MPa) to 93 ksi (639 MPa) after the thermal exposure. This is in sharp contrast to the other three alloys. For example, Waspaloy alloy originally had a yield strength of 99 ksi (682 MPa) which was higher than 282 alloy. However, after the thermal exposure at 1400°F (760°C), the yield strength fell to 80 ksi (549 MPa), which is considerably lower than that of 282 alloy. Likewise, the yield strength of 263 alloy, already well below that of 282 alloy, decreased further from 79 ksi (541 MPa) to 73 ksi (505 MPa) as a result of thermal exposure. Even R-41 alloy, which started out with a high yield strength of 113 ksi (777 MPa) in the as-age hardened condition, was found to lose strength after thermal exposure falling to 104 ksi (718 MPa). Therefore, only 282 alloy was found to actually increase in yield strength after long term exposure at 1400°F (760°C), a strong testament to the alloy's exceptional thermal stability.

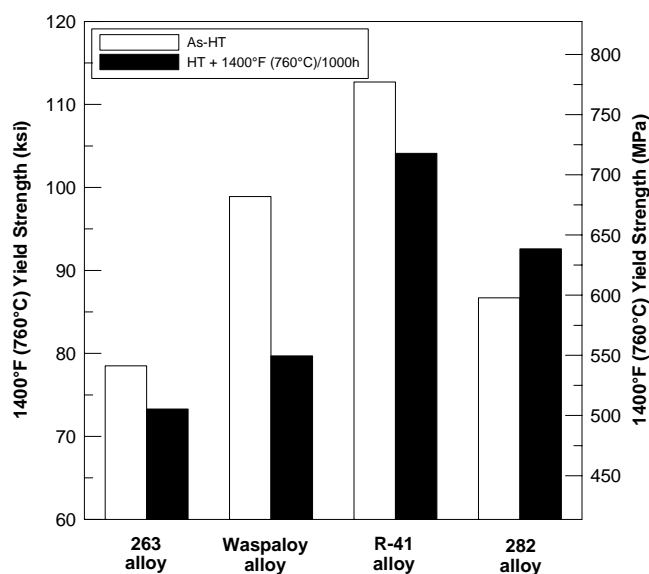


Fig. 17 Effect of thermal exposure on the yield strength *at the exposure temperature* of 1400°F (760°C)

## 7.0 Summary and Conclusions

The key metallurgical features of the new HAYNES 282 alloy were discussed along with the implications of these features on the principal attributes of the alloy, namely its combination of excellent creep strength and fabricability. Several observations and conclusions were made.

1. The microstructure of the as-heat treated 282 alloy, consisted of primary MC carbides and secondary  $M_{23}C_6$  carbides found intragranularly as well as along grain boundaries. The  $\gamma'$  phase consisted of a uniform distribution of fine, spherical precipitates approximately 20 nm in diameter.
2. The equilibrium  $\gamma'$  content in 282 alloy was chosen at an intermediate level to achieve a balance between fabricability and strength.
3. The sluggish  $\gamma'$  precipitation kinetics in 282 alloy are responsible for the alloy's proven resistance to strain-age cracking as well as its high formability in the solution annealed condition.
4. Despite a lower  $\gamma'$  content, the creep strength of 282 alloy was found to be better than that of Waspaloy alloy and approaching that of R-41 alloy. This can be attributed to a number of factors, including an optimized Mo content, lack of deleterious phase formation, and retention of high strength after aging, presumably a result of the resistance to  $\gamma'$  coarsening.
5. A number of other properties of 282 alloy, including tensile, LCF, and thermal stability, were presented along with comparative data for R-41, Waspaloy, and 263 alloys. It was found that 282 alloy possesses a unique combination of properties which makes it an outstanding candidate for a number of high temperature applications.

## Acknowledgments

The author would like to thank the many individuals in the Haynes International Technology Laboratories for tremendous efforts during both the alloy development and alloy characterization efforts.

## References

1. L.M. Pike, "HAYNES 282 Alloy - A New Wrought Superalloy Designed for Improved Creep Strength and Fabricability", *ASME Turbo Expo 2006*, Barcelona, Spain, Paper No. GT-2006-91204.
2. C.T. Sims, N.S. Stoloff, and W.C. Hagel, *Superalloys II*, (New York: John Wiley & Sons, 1987).
3. L.M. Pike and S. K. Srivastava, "Oxidation Behavior of Wrought Gamma-Prime Strengthened Alloys", *High-Temperature Corrosion and Protection of Materials 2008*, Les Embiez, France, 2008.
4. R.W. Fawley and M. Prager, "Evaluating the Resistance of Rene 41 to Strain-Age Cracking", *WRC Bulletin*, 150 (1970) 1-12.
5. M.D. Rowe, "Ranking the Resistance of Wrought Superalloys to Strain-Age Cracking", *Welding Journal*, 85(2) (2006), 7-s to 34-s.

6. M. Prager and C.S. Shira, *Weld. Res. Counc. Bull.*, 128 (1968).
7. W. Betteridge and J. Heslop, *The Nimonic Alloys* (New York: Crane Russak & Company, 1974).
8. L. M. Pike, "Low-Cycle Fatigue Behavior of HAYNES<sup>®</sup> 282<sup>®</sup> Alloy ", *ASME Turbo Expo 2007*, Montreal, Canada, Paper No. GT-2007-28267.
9. H.J. Beattie, and W.C. Hagel, "Intergranular Precipitation of Intermetallic Compounds in Complex Austenitic Alloys", *Trans. AIME*, 221 (1961) 28-34.
10. H.E. Collins, "Relative Stability of Carbide and Intermetallic Phases in Nickel Base Superalloys", *International Symposium on Structural Stability in Superalloys*, AIME High Temperature Alloys Committee Publication, Seven Springs, PA, (1968), 171-98.
11. H.E. Collins, "Relative Long-Time Stability of Carbide and Intermetallic Phases in Nickel Base Superalloys", *Trans. ASM*, 62 (1969) 82-104.